

5. Results

5.1 Virulent (LP) and avirulent (HP) *L. major* show differential gene expression

Previous pan-transcriptome analyses of 9000 genes identified those which were either up- or down-regulated in virulent and avirulent strains of *Leishmania* (5ASKH, LV39, Ag83 and LV9). Based on the FLAG value output and >2-fold change cut-off parameters, we selected 31 genes. We validated the results by qPCR of selected genes in promastigotes and amastigotes of each virulent and avirulent *Leishmania* strain and selected 20 genes showing alterations in expression similar to microarray analysis (**Table 6**).

Table 6. *In silico* analysis of leishmanial genes selected from qPCR

S. No.	Protein	% Identity (Mus musculus)	% identity (Homo sapiens)	Contiguous stretch of >11 similar amino acids
1.	DNA polymerase ϵ subunit B	26	25	No
2.	Pyruvate Carboxylase	29	30	No
3.	p-nitrosophenyl phosphatase	36	35	No
4.	Aldehyde dehydrogenase	46	48	Yes
5.	Coprophyrinogen III oxidase	45	46	Yes
6.	Fatty acid desaturase	44	46	Yes
7.	gp63 Leishmanolysin	27	24	No
8.	Methionine aminopeptidase	60	57	Yes
9.	NAD ⁺ synthase	26	22	No
10.	Thiol dependent reductase-1	24	33	No
11.	2-oxoisovalerate dehydrogenase	46	46	Yes
12.	Adenine phosphoribosyl transferase	47	42	Yes
13.	Adenylate kinase	37	46	No
14.	ARP 2/3 kinase	43	49	No
15.	Iron superoxide dismutase	38	41	Yes
16.	Phosphatidic acid phosphatase	40	36	No
17.	Ubiquitin conjugating enzyme E2	71	70	Yes
18.	LmjF_36_4610	39	42	No
19.	LmjF_36_3850	34	44	No
20.	LmjF_33_2620	33	32	No

In present study, to rule out probable auto-immune reaction elicited during vaccination regimen, *in silico* sequence alignment search of 20 genes with mouse and human proteome by blastp identified 12 genes which showed little or no similarity with mouse and human proteome (**Table 6**).

Finally, we analyzed the transcript-level expression of 12 genes in unstimulated and IFN- γ stimulated *L. major*-infected macrophages 8 hours post-infection. NAD⁺ synthase, adenylate kinase, LmjF_36_3850 (Lm₂), Phosphatidic acid phosphatase (PAP), Thiol-dependent reductase 1 (TDR1) and LmjF_33_2620 (Lm₁) were significantly down-regulated in unstimulated and IFN- γ stimulated HP-infected macrophages; while leishmanial n-nitrophenyl phosphatase (NPP), leishamanolysin (gp63), pyruvate carboxylase (Pyr Carb), hypoxanthine guanine phosphoribosyl transferase (HGPRT) and ARP 2/3 complex 16 KDa subunit (ARP2/3) were significantly up-regulated in unstimulated and IFN- γ stimulated *L. major*-infected macrophages. In fact, we observed no detectable expression of NAD⁺ synthase and adenylate kinase in HP-infected macrophages. Similarly, no detectable expression of n-nitrophenyl phosphatase and gp63 was observed in LP-infected macrophages. No significant difference in expression levels of DNA polymerase epsilon subunit B (DNA Pol) was observed between LP- and HP-infected macrophages (**Figure 7**). Thus, we concluded that the genes whose expression levels are higher in virulent form of parasite in unstimulated or IFN- γ stimulated condition (a stress condition for *Leishmania*) could be probable virulence factors in *Leishmania* sp. and serve as potential vaccine candidates against leishmaniasis.

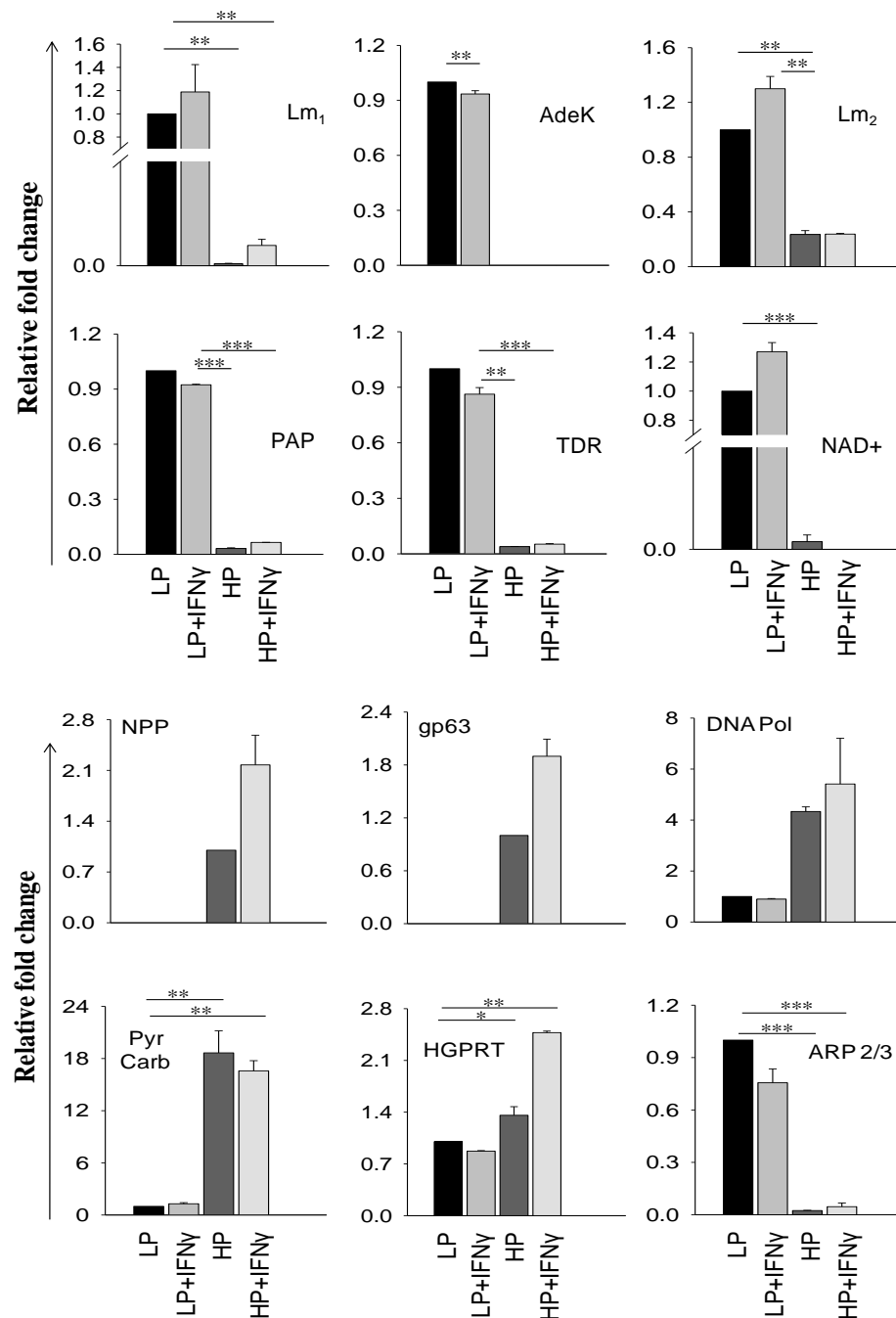


Figure 7. Relative expression of leishmanial genes in virulent and avirulent *L. major* infected BALB/c mice. Thioglycollate-elicited peritoneal macrophages were infected with *L. major* promastigotes (1:10 ratio, 6h). Infected macrophages were stimulated with rIFN- γ or not for 8h. (***, $p \leq 0.001$, **, $p \leq 0.01$, *, $p \leq 0.05$, ns indicates $p \geq 0.05$; $n=3$). Data is represented as Mean \pm SEM and representative of three independent experiments.

5.2 LmjF_36_3850 is expressed *in vitro*, *in vivo* and is able to produce anti-LmjF_36_3850 IgG upon vaccination

To test the efficacy as a DNA vaccine candidate, LmjF_36_3850 was cloned in pcDNA6/HisA vector. Successful ligation was confirmed by restriction digestion of positive colonies (**Figure 8a**) and sanger sequencing, which confirmed the sequence integrity and in-frame cloning of insert. Cloned vector (Leish-pcDNA) transfected into HEK293T cells and injected into left thigh muscle (i.m.) expressed LmjF_36_3850 transcripts (**Figure 8b, c**).

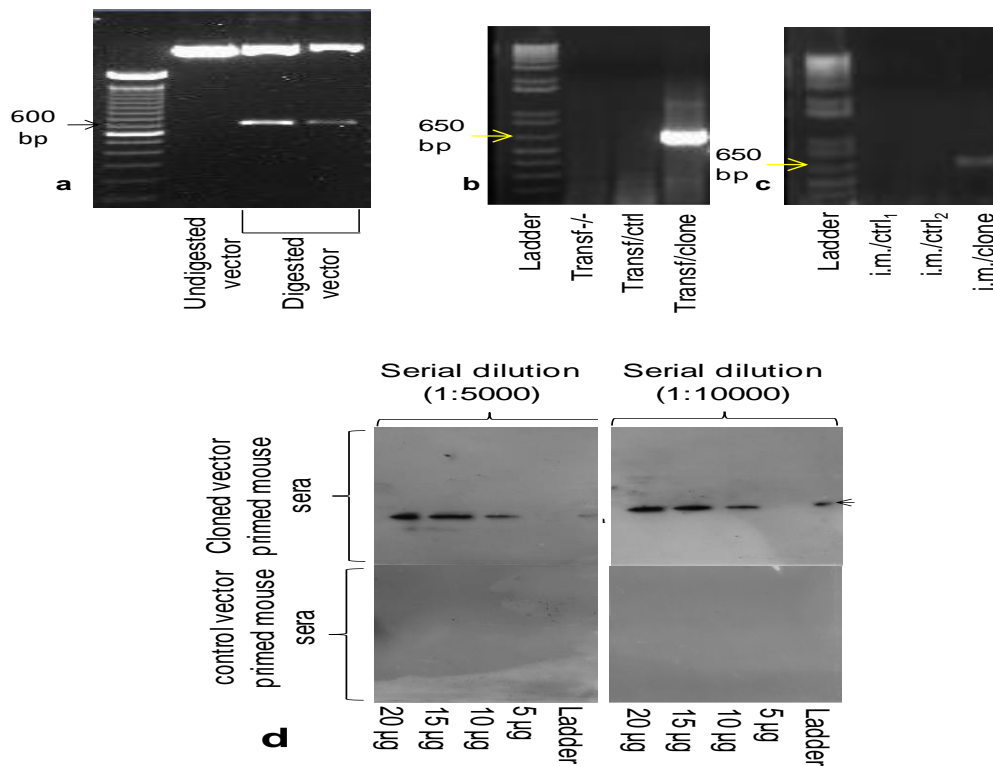


Figure 8. PCR-based cloning of LmjF_36_3850, *in vivo* and *in vitro* expression. (a) LmjF_36_3850 was cloned in pcDNA6/HisA vector between BamHI and XbaI cloning sites. Lm-pcDNA was transfected into (b) HEK293T and (c) injected i.m. in left thigh. Transcript levels of LmjF_36_3850 were checked 48h post-transfection and 4 days post-injection.

5.3 LmjF_36_3850 vaccination elicits anti-LmjF_36_3850 IgG antibodies and is unable to curb disease progression and parasite load

DNA vaccination with LmjF_36_3850 induces a significantly higher titer of anti-leishmanial IgG2a antibodies as compared to control and naïve mice. Also, anti-leishmanial IgG1 antibody titre was also found to be higher in vaccinated mice as compared to control groups (**Figure 9a**). Hence, IgG2a/IgG1 ratio, which indicates Th1-biased response, is comparable among the groups and approximately equals to 1 (**Figure 9b**). Hence, LmjF_36_3850 vaccination induces a mixed Th1/Th2 response. Also, levels of IgM were comparable in all groups. Moreover, serum obtained from vaccinated mice was able to detect LmjF_36_3850 in virulent *L. major* lysate, indicating that antigen is immunogenic and elicited IgG antibodies are antigen-specific (**Figure 8d**). Furthermore, vaccinated mice were unable to control lesion progression after *L. major* challenge as we observed comparable footpad thickness in vaccinated and control mice (**Figure 9c**). Lymph node hypertrophy was also statistically insignificant between the groups. Moreover, we observed higher, albeit insignificant, parasite burden in draining lymph node (dLN) of control vector-injected and Leish-pcDNA vaccinated mice as compared to saline-injected mice post-challenge infection (**Figure 9d, 9e**).

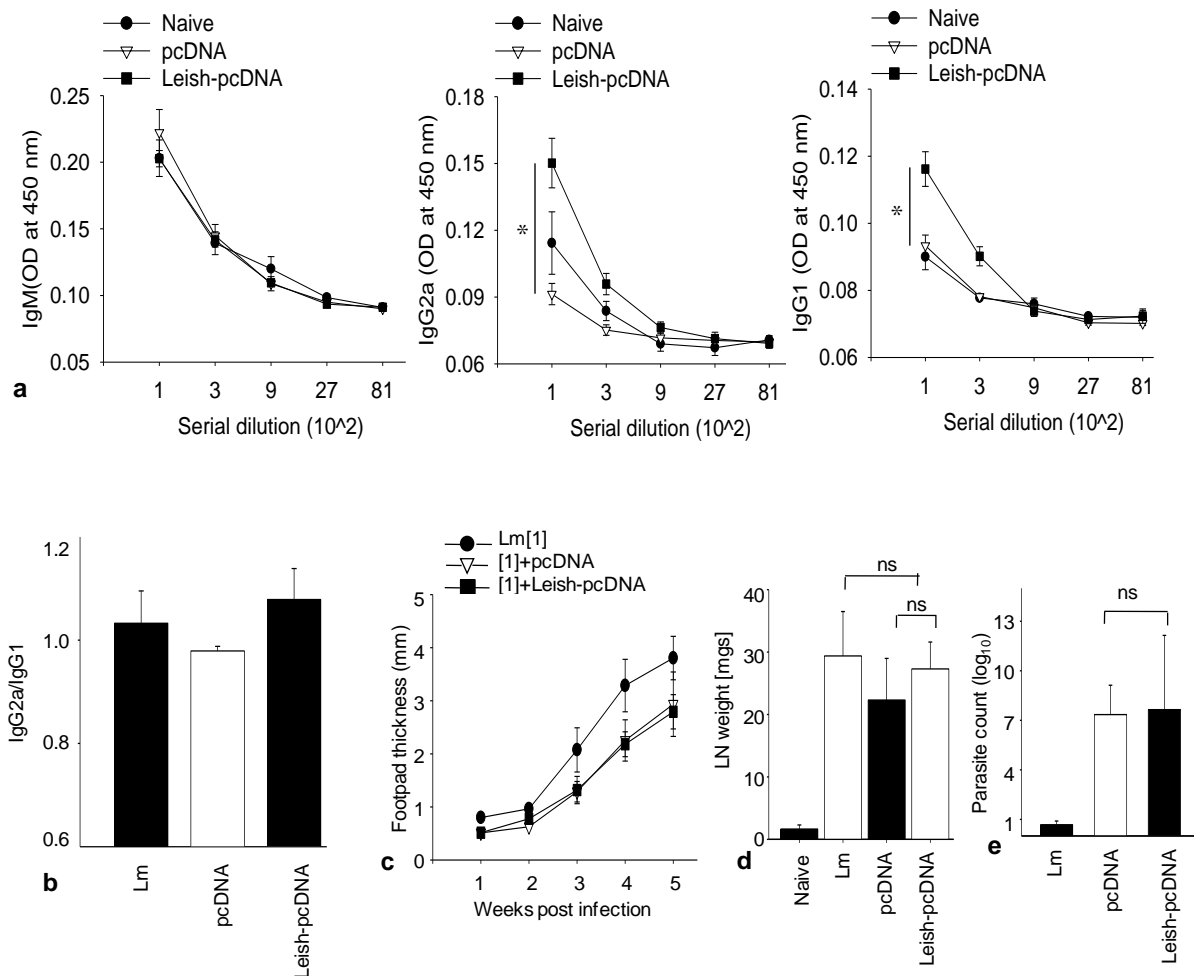


Figure 9. DNA immunization with LmjF_36_3850 elicits mixed Th response and does not control lesion progression and parasitic load. (a) Anti-leishmanial IgM, IgG2a, IgG1 were assessed in blood sera from different groups of mice by ELISA (OD = 450 nm). (b) IgG2a/IgG1 ratio was calculated from respective IgG absorbance readings. (c) Mean footpad thickness during the course of infection in different groups of mice (d) Draining Lymph node (popliteal) weight and, (e) Parasite load after 5 weeks of challenge infection in different groups of mice. Data is represented as Mean±SEM. (***) indicates $p \leq 0.001$, ** indicates $p \leq 0.01$, * indicates $p < 0.05$, ns indicates $p \geq 0.05$; $n=5$). Data is representative of two independent experiments.

5.4 Lymphocytes from vaccinated mice show anti-inflammatory, Th2 cytokine signatures and sera from vaccinated mice contain higher anti-leishmanial IgG1 antibodies post-challenge infection

Lymphocytes from dLN of vaccinated mice have higher expression levels of pro-parasitic Th2 and Treg cytokines such as IL-4 and IL-10 respectively. Also, FOXP3 levels were higher in vaccinated mice, which is a signature transcription factor of Treg cells. However, we did not observe any significant change in IFN- γ and IL-17 levels (**Figure 10a**). Upon re-stimulation with crude soluble antigen (CSA) of *L. major*, lymphocytes from vaccinated mice secreted lower IFN- γ than controls and IL-10 levels of vaccinated mice were comparable to saline-injected *L. major*-infected mice. Although secreted IL-4 was lower than control-vector injected mice, it was still significantly higher than saline-injected mice (**Figure 10b**). Moreover, sera from vaccinated mice contained significantly high anti-leishmanial IgG1 levels than the control groups. IgG2a levels were also higher in vaccinated mice, although it was not statistically significant. Thus, IgG2a/IgG1 ratio is higher in vaccinated mice than control mice but the immune response was skewed towards Th2 subtype (IgG2a/IgG1<1) (**Figure 10c**).

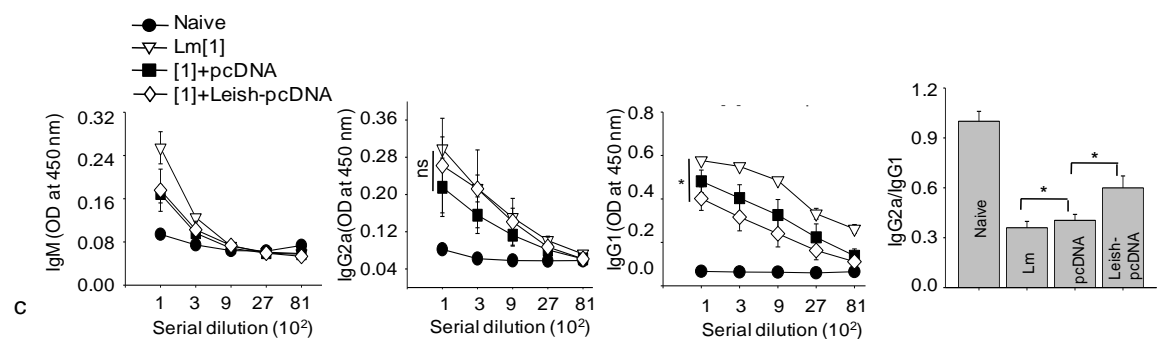
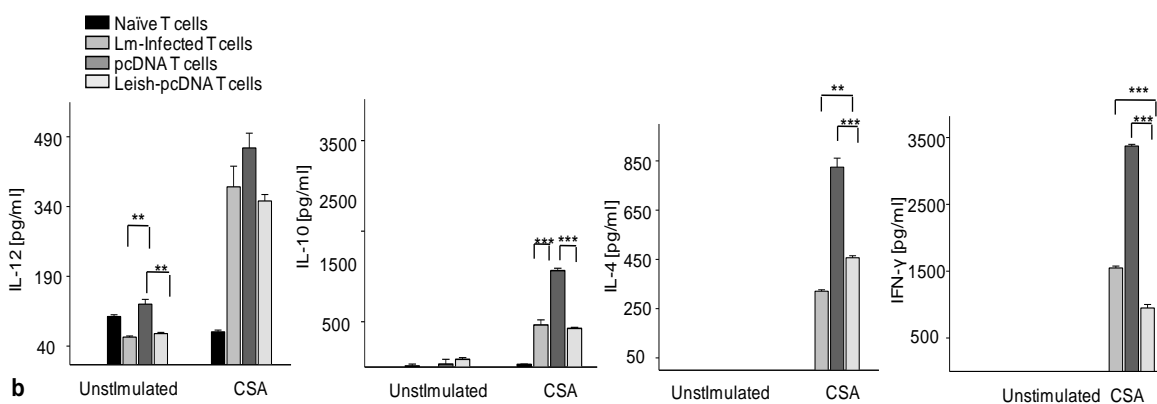
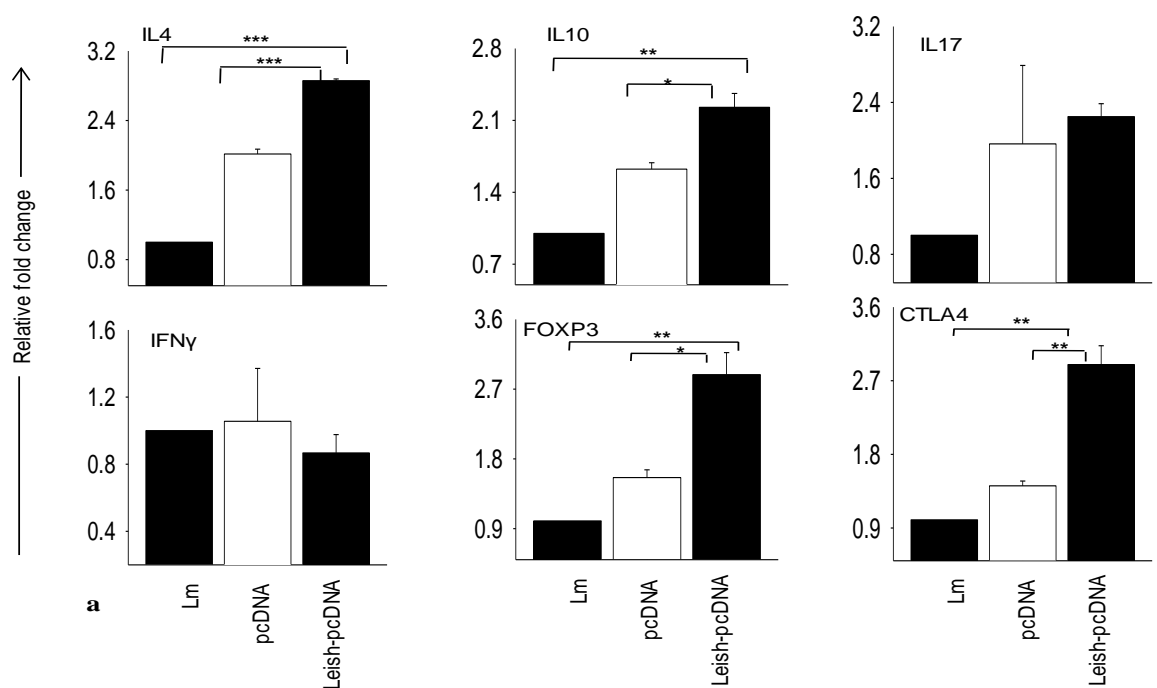


Figure 10. DNA vaccinated mice had higher population of anti-inflammatory cytokine secreting cells and elevated IgG1 levels post-infection. (a) Lymphocytes from dLN of different groups were lysed and total RNA was extracted. Relative quantitative levels of IL-4, IL-10, IFN γ , IL-17, IL-12, FOXP3, and CTLA4 were analysed by qPCR. (b) Lymph node cells were either kept unstimulated or stimulated by *L. major* CSA (30 μ g/ml) and cytokine quantitation in culture supernatant was done by ELISA after 72 h. (OD = 450 nm). (c) Anti-leishmanial IgM, IgG2a, IgG1 levels in sera were estimated by ELISA (OD = 450 nm) and IgG2a/IgG1 ratio was calculated. Data is represented as Mean \pm SEM.(*** indicates $p\leq 0.001$, ** indicates $p\leq 0.01$, * indicates $p<0.05$, ns indicates $p\geq 0.05$; n=5). Data is representative of two independent experiments.

5.5 Lymphocytes from vaccinated mice had higher levels of IgG1 and IgG2a secreting

B cells

B220+ CD19+ B lymphocyte population from vaccinated group had higher percentage of IgG2a secreting cells than the control group, although IgG2a secreting B cell population in saline-injected mice was comparable to the vaccinated mice. Similarly, IgG1 secreting B cells were higher than control-vector injected group and comparable to saline-injected group (**Figure 11**). This observation corroborates with IgG levels observed in sera from different groups of mice.

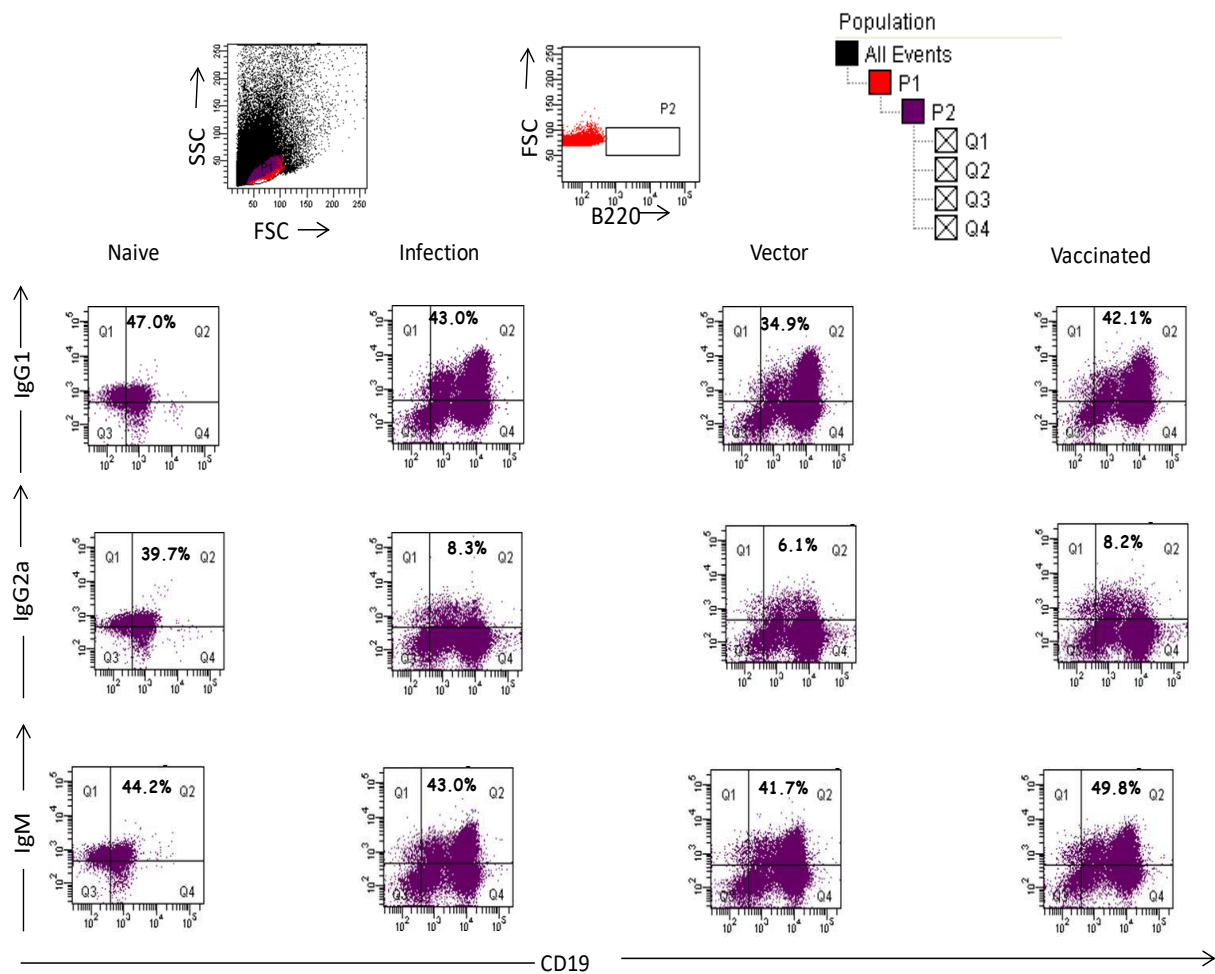


Figure 11. Flow cytometry analysis of Ig-specific B cell subsets in draining lymph nodes of indicated groups of mice. 2×10^6 lymphocytes/group were stained with FITC-anti-B220, PE-anti-CD19, biotinylated anti-IgM, anti-IgG2a, anti-IgG, and V450 conjugated streptavidin and events were recorded and analyzed.

5.6 Lymphocytes from vaccinated mice had higher population of pro-leishmanial Th2 and Treg memory cells

CD44^{hi} CD62L^{lo} (T_{EM}) compartment of vaccinated mice had higher population of GATA3+ IL-4 and RORγt+ IL-17 secreting cells than the control groups. Also, FOXP3+ IL-10 secreting Treg-TEM cells were higher in vaccinated mice, while tbet+ IFN-γ

secreting Th1-TEM cells were lower in vaccinated mice than the control groups (**Figure 12**). T_{CM} compartment, which acts as reservoir of antigen-specific T cells for long-term immune response, was also skewed towards the pro-leishmanial Th cells. Population of $CD44^{hi} CD62L^{hi}$ CD4 T cells had higher population of GATA3+ IL-4+, $ROR\gamma t^{+}$ IL-17+ and FOXP3+ IL-10+ T_{CM} cells, although $tbet^{+}$ IFN- γ^{+} T_{CM} cells were found to be higher in vaccinated group as compared to control mice (**Figure 13**). These results indicate that DNA vaccination with LmjF_36_3850 skews the Th memory compartment towards anti-inflammatory Th2, Th17 and Treg subtypes, and thus helping in parasite persistence.

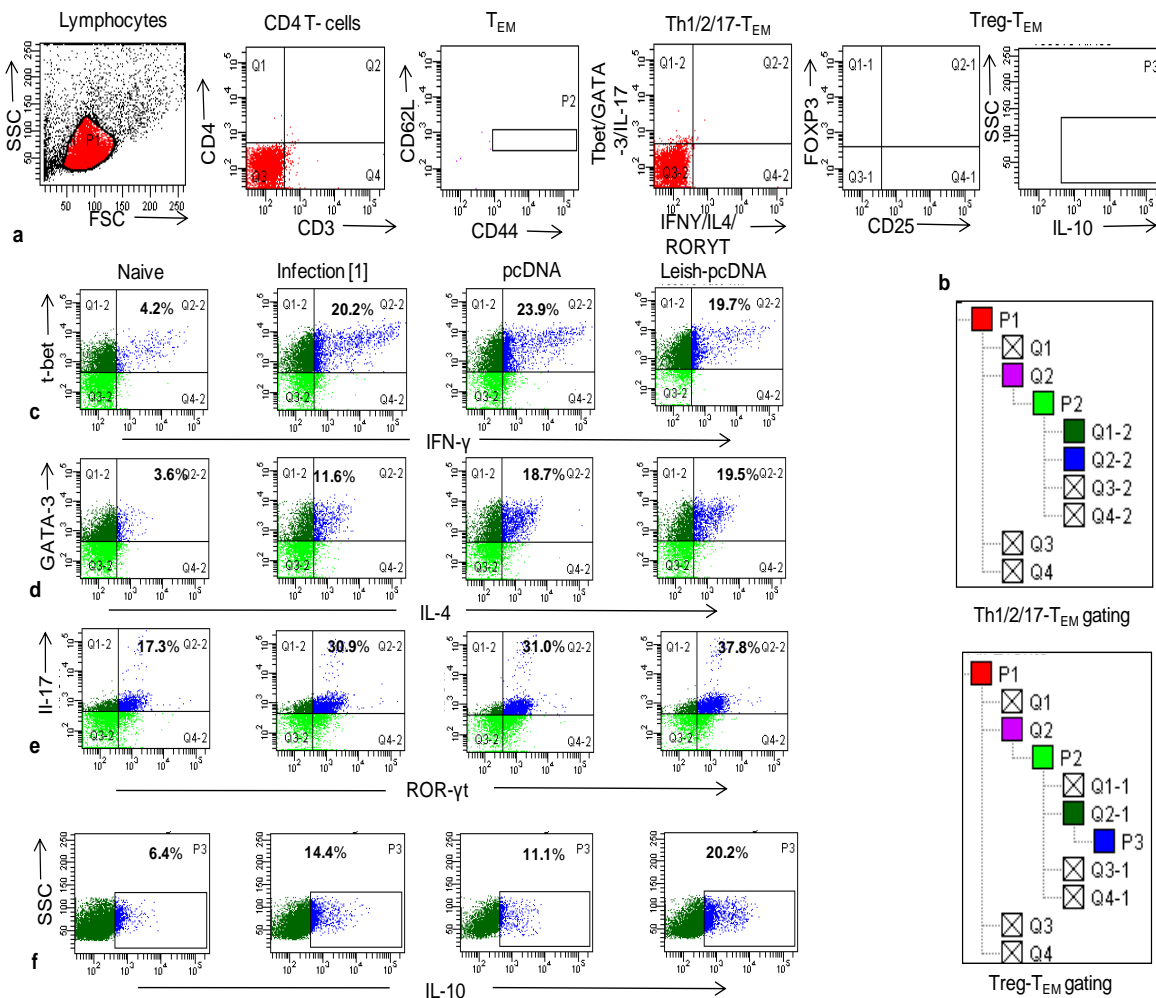


Figure 12. Lymphocytes from vaccinated mice contain a higher repertoire of Th2, Th17 and Treg- T_{EM} cells. (a) and (b) Gating strategy (isotype staining population is shown) used to analyze the T_{EM} cells from draining lymph node. (c), (d), (e) and (f) Lymphocytes from each mice in a group were pooled together (n=5) and IFN- γ , IL-4, IL-17 and IL-10 secreting Th1-, Th2-, Th17- and Treg- T_{EM} cell population were determined from indicated groups of mice. Data is representative of two independent experiments.

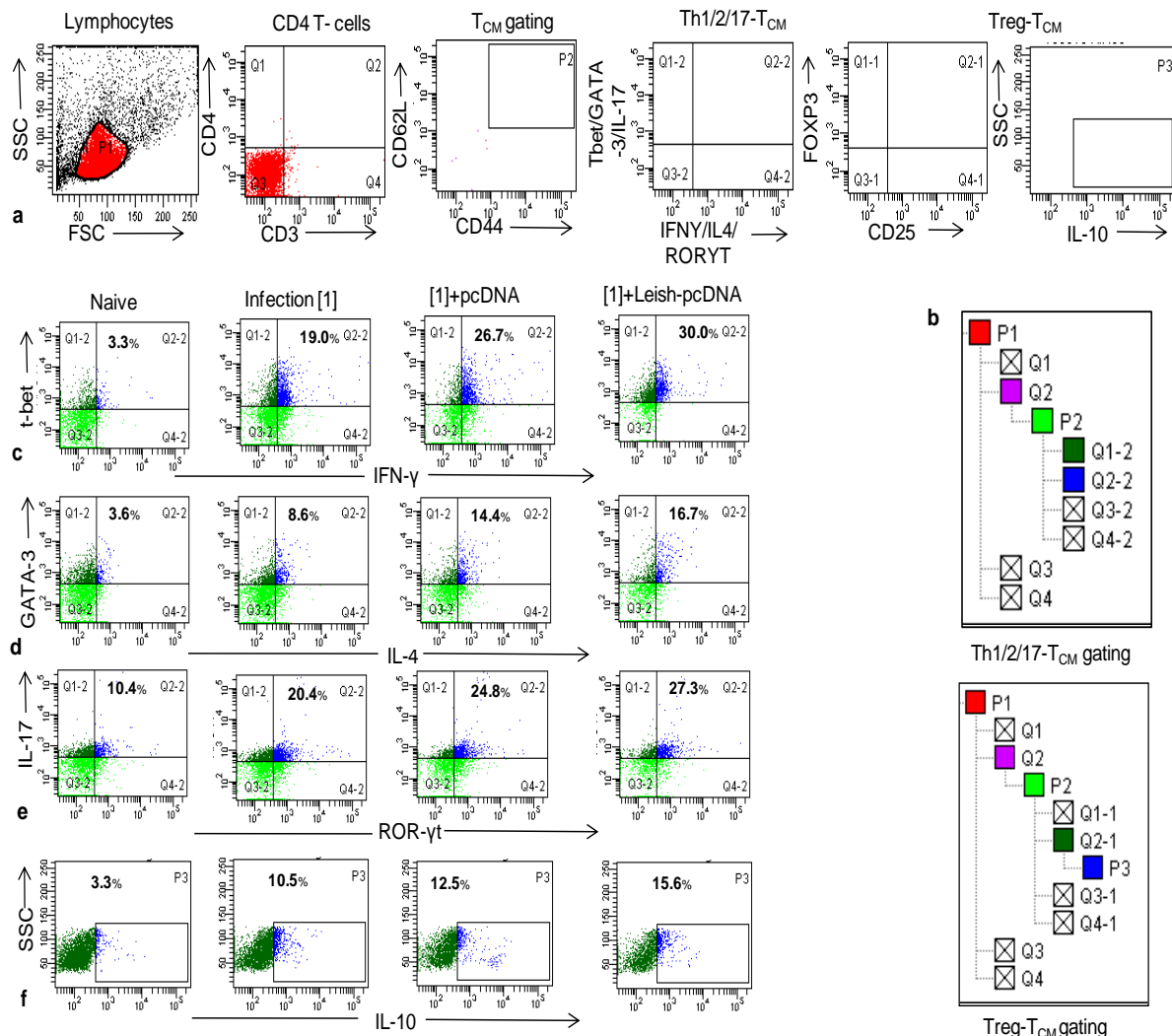


Figure 13. Lymphocytes from vaccinated mice contain a higher repertoire of Th2, Th17 and Treg- T_{CM} cells. (a) and (b) Gating strategy (isotype staining population is shown) used to analyze the T_{CM} cells from draining lymph node. (c), (d), (e) and (f) Lymphocytes from each mice in a group were pooled together (n=5) and IFN- γ , IL-4, IL-17 and IL-10 secreting Th1-, Th2-, Th17- and Treg- T_{CM} cell population were determined from indicated groups of mice. Data is representative of two independent experiments.

5.7 Cloning, *in vitro* and *in vivo* expression and purification of *L. major* adenylate kinase (LmAdeK)

Adenylate kinase was also observed to be significantly down-regulated in non-virulent *L. major*-infected macrophages. Hence, we selected LmAdeK for vaccination trial using heterologous prime-boost (HPB) strategy. We cloned LmAdeK into pcDNA6/HisA and pet28a+ vector and confirmed the successful insertion by double-digestion using restriction enzymes (**Figure 14a**) and sanger sequencing. LmAdeK-pcDNA (LmpcDNA) expression was observed 48 hours post-transfection in HEK293T cell line and 4 days post-i.m. injection in left thigh, which suggests that LmpcDNA construct was able to express insert *in vitro* and *in vivo* (**Figure 14b**).

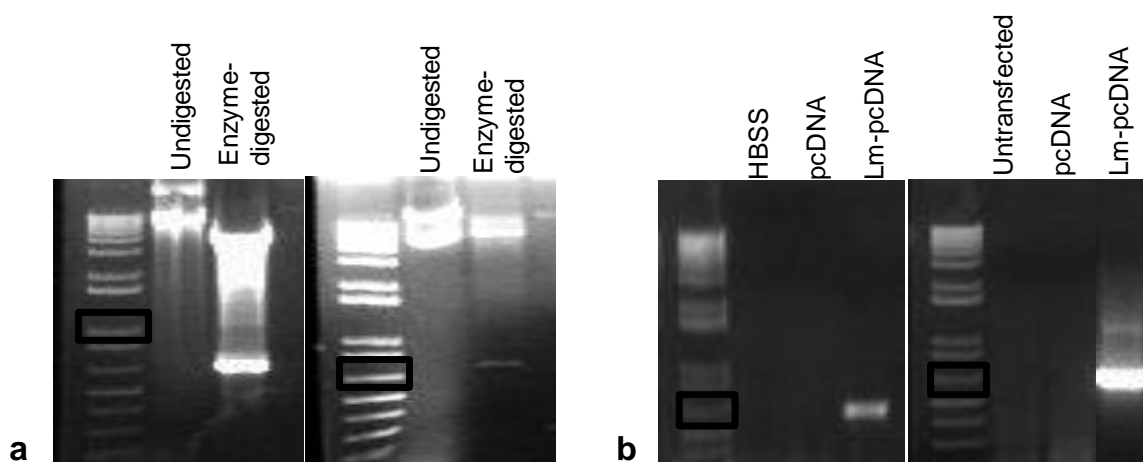


Figure 14. Cloning of *L. major* adenylate kinase, *in vivo* and *in vitro* expression of pcDNA construct. (a) LmAdeK is cloned in pcDNA6/HisA (left) and pet28a+ (right) and confirmed by restriction digestion and sanger sequencing of positive plasmids. (b) 100 μ g LmpcDNA was injected in left thigh muscle (left) and transfected into HEK293T (right) and LmAdeK expression levels were determined 4 days post-injection and 48 h post-transfection respectively. (Indicated box shows 650 bp DNA marker).

5.8 Purification of recombinant *L. major* adenylate kinase

IPTG induction and purification with affinity-based chromatography yielded pure fractions containing recombinant *L. major* adenylate kinase (rAdeK) without any significant contaminating bands observed in Coomassie dye staining or silver staining (**Figure 15a-c**). It was dialyzed to remove unwanted chemical agents used during purification process. Different concentrations of purified protein was recognized by anti-His tag antibody and *L. major* infected mouse sera which suggests that purified protein is indeed rAdeK and is immunogenic in natural infection settings and host elicits anti-AdeK IgG antibodies (**Figure 15d**).

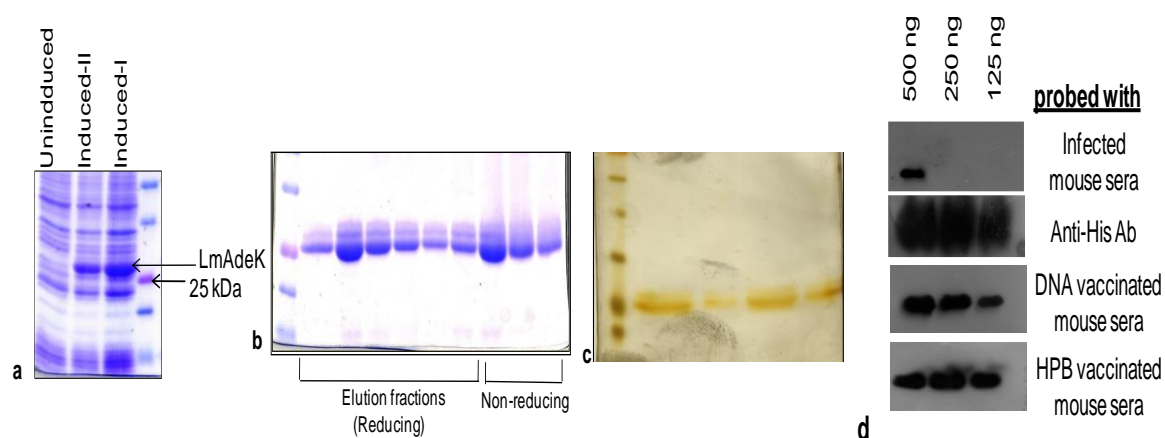
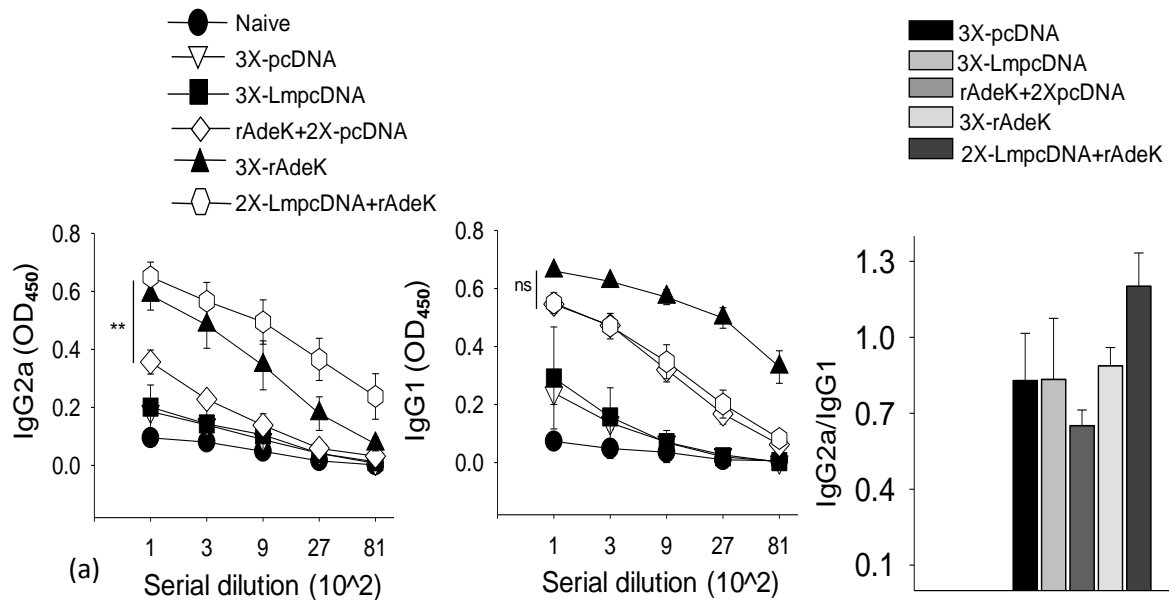


Figure 15. IPTG-based heterologous expression and affinity-based purification of recombinant LmAdeK (rAdeK). (a) LmAdeK-pet28a+ was transformed into BL-21(RIL) and protein induction was done by 0.1 mM IPTG, 18°C. (b) Recombinant protein was eluted with 300mM imidazole from Ni-NTA beads by His-tag affinity purification as indicated in material and methods and purity was confirmed by (c) silver staining. (d) Recombinant protein was probed by anti-His tag antibody, *L. major* infected mouse sera, DNA vaccinated and HPB vaccinated mouse sera to confirm the immunogenicity of LmAdeK during natural infection and vaccination regimen.

5.9 HPB vaccination with LmAdeK elicits higher IgG2a antibodies pre- and post-challenge infection

Four weeks post-vaccination, HPB and 3X-rAdeK vaccinated mice elicited significantly higher anti-AdeK IgG2a levels than other groups. HPB vaccinated mice elicited lower anti-AdeK IgG1 levels than 3X-rAdeK vaccinated mice, although the difference between the groups was not significant. IgG2a/IgG1 ratio, an indicator of Th1-biased immune response, was higher in HPB vaccinated mice than other groups and it was >1 (**Figure 16a**). It indicates that HPB vaccination induces Th1-biased immune response. Also, HPB and 3X-rAdeK vaccinated mice retained higher anti-AdeK IgG2a levels than other vaccinated and control groups five weeks post-challenge infection. Although IgG1 levels in HPB vaccinated group were lower than 3X-rAdeK and 1X-rAdeK vaccinated group, the difference was not statistically significant (**Figure 16b**). IgG2a/IgG1 ratio in HPB vaccinated group was still higher than other groups' five-weeks post *L. major* infection.



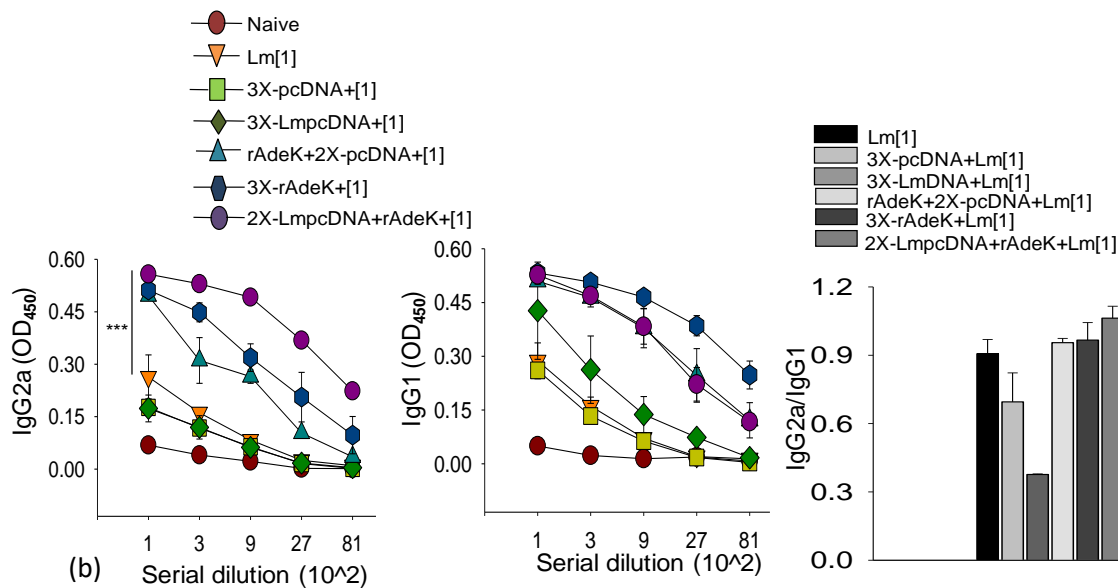


Figure 16. HPB vaccination increases the anti-LmAdeK IgG2a levels and skews response towards Th1 subtype. Anti-LmAdeK IgG2a and IgG1 levels were determined from sera of different groups of mice after (a) 4 weeks of last vaccination and (b) 5 weeks post-challenge infection. IgG2a/IgG1 ratio was calculated from the absorbance reading of the lowest serum dilution in each group. Data is represented as Mean±SEM. (***) indicates $p \leq 0.001$, ** indicates $p \leq 0.01$, * indicates $p < 0.05$, ns indicates $p \geq 0.05$; $n=5$). Data is representative of two independent experiments.

5.10 HPB vaccination with LmAdeK was able to decrease cutaneous lesion progression and parasitic load

HPB vaccinated mice have lower footpad thickness at the site of infection than other vaccinated groups after 5 weeks of challenge infection (**Figure 17a**). Also, the parasitic load in the dLN was lower in HPB and 3XrAdeK vaccinated group as compared to 1XrAdeK and 3XLmpcDNA vaccinated mice (**Figure 17b, c**). Although the parasitic load of HPB and 3XrAdeK mice were comparable, decreased lesion progression by HPB vaccination suggests a better resolution of pathological symptoms.

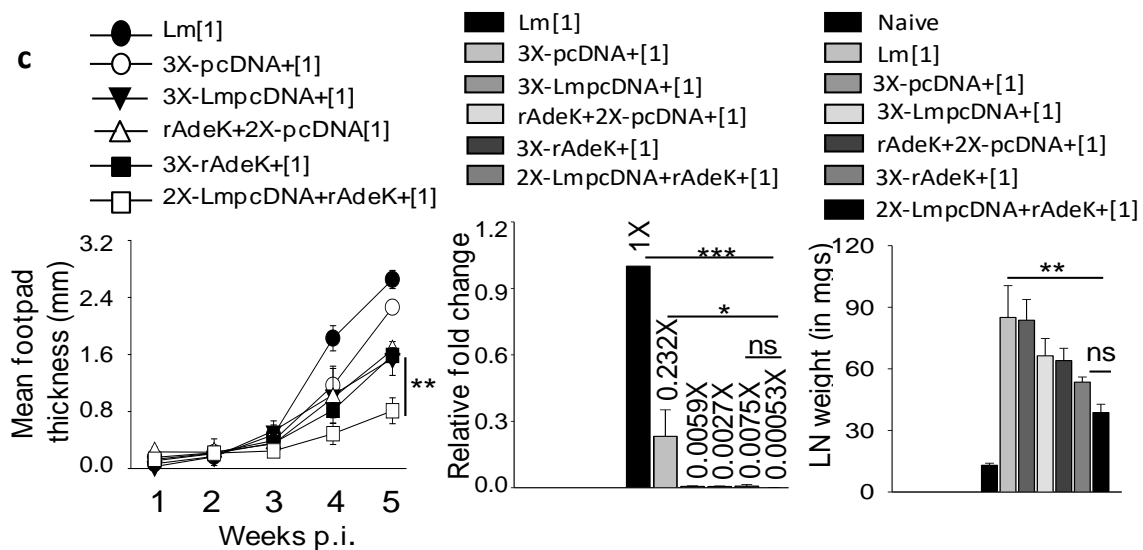


Figure 17. HPB vaccination with LmAdeK controls the progression of cutaneous lesion, lymph node hypertrophy and parasite load in draining lymph node. (a) Mean footpad thickness during the course of infection in different groups of mice (b) Draining Lymph node (popliteal) weight and, (c) Parasite load after 5 weeks of challenge infection in different groups of mice. Data is represented as Mean \pm SEM of fold-decrease in parasite count in different groups as compared to control group [Lm] (***) indicates $p \leq 0.001$, ** indicates $p \leq 0.01$, * indicates $p < 0.05$, ns indicates $p \geq 0.05$; $n=5$). Data is representative of two independent experiments.

5.11 Lymphocytes from HPB vaccinated mice have higher IFN- γ producing and lower IL-4, IL-10 producing cells

qPCR analysis of effector cytokines in lymphocytes from vaccinated and control groups suggests that HPB vaccinated mice had significantly higher levels of anti-leishmanial IFN- γ containing cells than other groups. IL-4 levels remain undetectable in HPB- and 3X-rAdeK vaccinated mice. Although there was no significant difference in IL-10 levels between HPB vaccinated and 1XrAdeK vaccinated group, CTLA-4 levels remained undetectable in HPB- and 3X-rAdeK vaccinated mice (**Figure 18**). This indicates a

dampened immunosuppressive and an enhanced inflammatory cytokine profile in draining lymph node from HPB vaccinated mice.

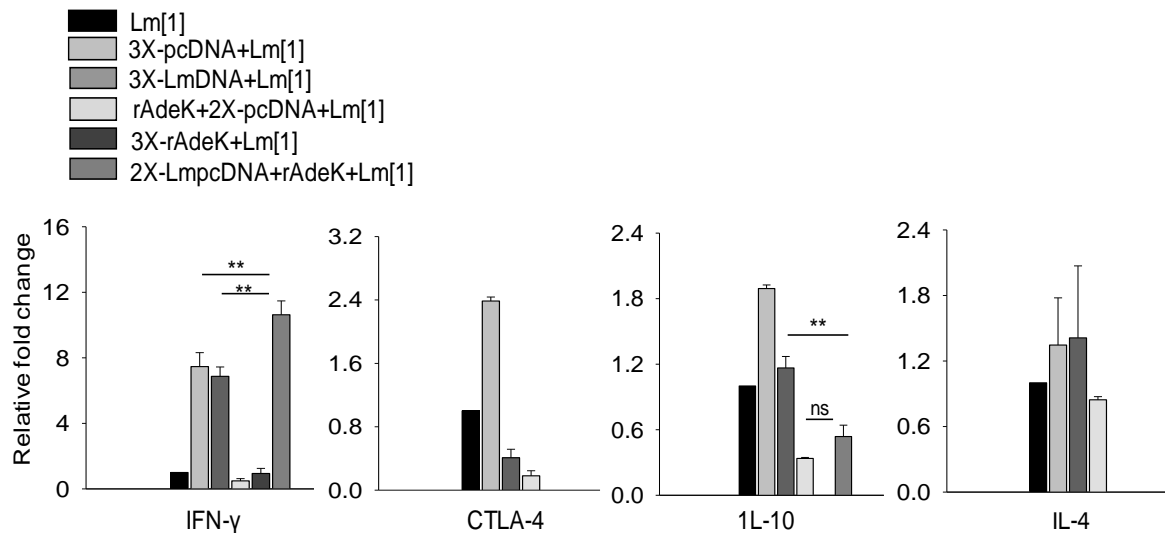


Figure 18. HPB vaccinated mice had higher levels of IFN- γ and lower expression of IL-10, IL-4 and CTLA-4 after 5 weeks of challenge infection. Lymphocytes from draining popliteal lymph node were lysed and transcript-expression of Th1- and Th2- based cytokines and co-inhibitory molecules were assessed by qPCR. Data is represented as Mean \pm SEM between duplicates. (***) indicates $p \leq 0.001$, ** indicates $p \leq 0.01$, * indicates $p < 0.05$, ns indicates $p \geq 0.05$). Data is representative of two independent experiments (n=5).

5.12 HPB vaccinated mice have less number of Th2, Th17 and Treg memory T cells

Flow cytometric analysis of Th-memory compartments revealed that CD4⁺ T cells from HPB vaccinated mice have less number of IL-4 secreting T_{CM}-Th2 memory cells. IL-4 secreting T_{EM}-Th2 memory cells were fewer in HPB vaccinated groups than in DNA vaccinated group and controls, but was comparable to 3XrAdeK and lower than 1XrAdeK vaccinee (**Figure 19e, f**). Th17-T_{EM}, Th17-T_{CM} and IL-10 secreting Treg-T_{EM} were lower in HPB vaccinated group as compared to other groups (**Figure 19g-i**). However, IFN- γ

secreting Th1-T_{EM} and Th1-T_{CM} were lower in HPB vaccinated group as compared to 3XrAdeK- and 1XrAdeK vaccinated group (**Figure 19c, d**).

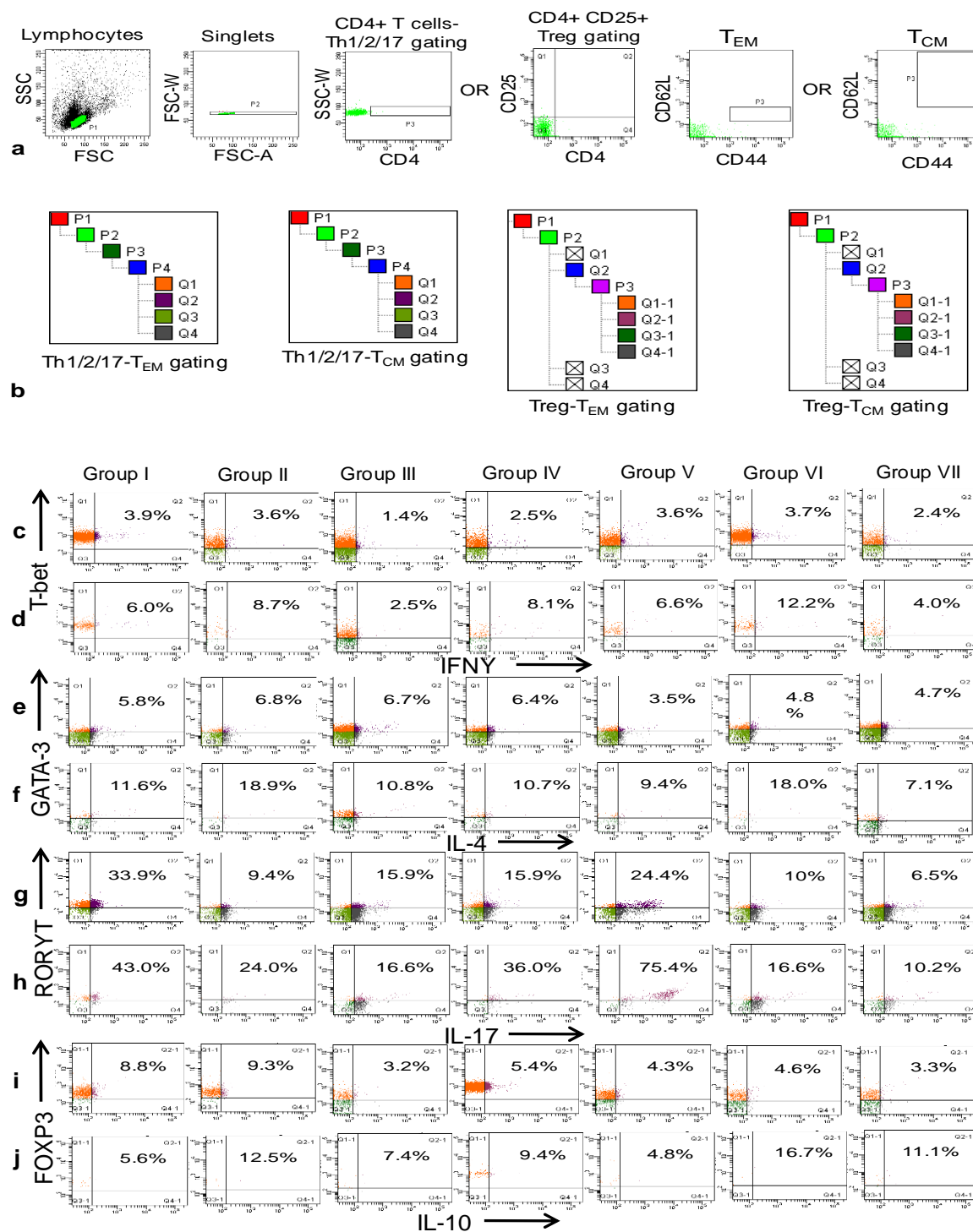


Figure 19. Lymphocytes from HPB vaccinated mice contain lower population of Th2, Th17 and Treg memory cells. (a) and (b) Gating strategy (isotype staining population is shown) used to analyze Th1, Th2, Th17 and Treg-T_{EM} and T_{CM} cells from draining lymph node. Lymphocytes from each mice in a group were pooled together (n=5) and IFN- γ , IL-4, IL-17 and IL-10 secreting (c, e, g and i) Th1-, Th2-, Th17- and Treg-T_{EM} cell population and (d, f, h, j) Th1-, Th2-, Th17- and Treg-T_{CM} cell population were determined from indicated groups of mice. Group nomenclature is described in materials and methods. Data is representative of two independent experiments (n=5).

These results suggests that HPB vaccinated mice have a lower repertoire of anti-inflammatory Th2, Th17 and Treg memory cells, although Th1 memory cells were also observed to be in lower number.

To summarize the data, we observed differential gene expression in the virulent and avirulent strain of *L. major*. Based upon that, we identified virulent factors of *Leishmania* which can be potential vaccine candidates against *L. major*. Hence, we cloned LmjF_36_3850 in pcDNA6/HisA and tested the efficacy of DNA vaccination and observed that immunization with LmjF_36_3850 induces a mixed Th response and is unable to curb the progression of infection and parasite load in dLN. Moreover, vaccinated mice had higher secretory levels and repertoire of anti-inflammatory cytokines and memory T cells respectively. Also, we cloned another virulence factor, LmAdeK, in pcDNA6/HisA and pet28a+ and tested various vaccination strategies and observed that HPB strategy was better in inducing a Th1-biased immune response upon vaccination and controlling the disease pathology. Also, HPB vaccinated mice had higher IFN- γ and lower IL-4, IL-10 secreting lymphocytes and lower population of anti-inflammatory, pro-leishmanial memory T cells than other vaccination strategies. We conclude that vaccination strategy play an important role in defining the outcome of vaccination.